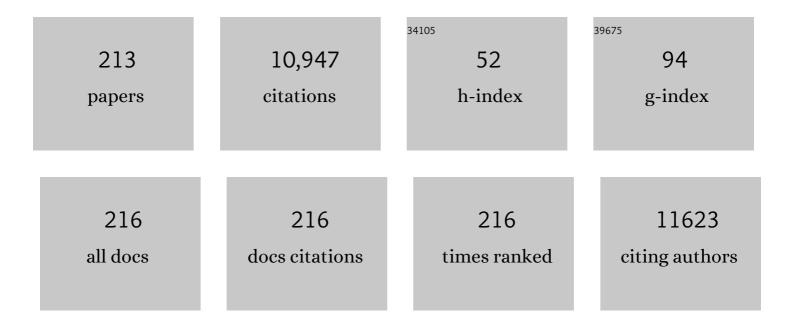
Chun-Sheng Shi

List of Publications by Year in descending order

Source: https://exaly.com/author-pdf/8795935/publications.pdf Version: 2024-02-01



#	Article	IF	CITATIONS
1	Carbon-Encapsulated Fe ₃ O ₄ Nanoparticles as a High-Rate Lithium Ion Battery Anode Material. ACS Nano, 2013, 7, 4459-4469.	14.6	937
2	Graphene Networks Anchored with Sn@Graphene as Lithium Ion Battery Anode. ACS Nano, 2014, 8, 1728-1738.	14.6	615
3	2D Space-Confined Synthesis of Few-Layer MoS ₂ Anchored on Carbon Nanosheet for Lithium-Ion Battery Anode. ACS Nano, 2015, 9, 3837-3848.	14.6	552
4	Ultrathinâ€Nanosheetâ€Induced Synthesis of 3D Transition Metal Oxides Networks for Lithium Ion Battery Anodes. Advanced Functional Materials, 2017, 27, 1605017.	14.9	284
5	Thermal decomposition-reduced layer-by-layer nitrogen-doped graphene/MoS2/nitrogen-doped graphene heterostructure for promising lithium-ion batteries. Nano Energy, 2017, 41, 154-163.	16.0	191
6	Porous MoS ₂ /Carbon Spheres Anchored on 3D Interconnected Multiwall Carbon Nanotube Networks forÂUltrafast Na Storage. Advanced Energy Materials, 2018, 8, 1702909.	19.5	190
7	A Topâ€Down Strategy toward SnSb Inâ€Plane Nanoconfined 3D Nâ€Doped Porous Graphene Composite Microspheres for High Performance Naâ€ion Battery Anode. Advanced Materials, 2018, 30, 1704670.	21.0	183
8	A nanosized SnSb alloy confined in N-doped 3D porous carbon coupled with ether-based electrolytes toward high-performance potassium-ion batteries. Journal of Materials Chemistry A, 2019, 7, 14309-14318.	10.3	157
9	CeO _{<i>x</i>} -Decorated NiFe-Layered Double Hydroxide for Efficient Alkaline Hydrogen Evolution by Oxygen Vacancy Engineering. ACS Applied Materials & Interfaces, 2018, 10, 35145-35153.	8.0	156
10	Rational design of Co9S8/CoO heterostructures with well-defined interfaces for lithium sulfur batteries: A study of synergistic adsorption-electrocatalysis function. Nano Energy, 2019, 60, 332-339.	16.0	156
11	Nâ€Doped Graphene Modified 3D Porous Cu Current Collector toward Microscale Homogeneous Li Deposition for Li Metal Anodes. Advanced Energy Materials, 2018, 8, 1800914.	19.5	155
12	Porous Graphitic Carbon Nanosheets as a High-Rate Anode Material for Lithium-Ion Batteries. ACS Applied Materials & Interfaces, 2013, 5, 9537-9545.	8.0	154
13	2D sandwich-like carbon-coated ultrathin TiO2@defect-rich MoS2 hybrid nanosheets: Synergistic-effect-promoted electrochemical performance for lithium ion batteries. Nano Energy, 2016, 26, 541-549.	16.0	146
14	A powder-metallurgy-based strategy toward three-dimensional graphene-like network for reinforcing copper matrix composites. Nature Communications, 2020, 11, 2775.	12.8	137
15	Controllable graphene incorporation and defect engineering in MoS2-TiO2 based composites: Towards high-performance lithium-ion batteries anode materials. Nano Energy, 2017, 33, 247-256.	16.0	130
16	Fabrication of in-situ grown graphene reinforced Cu matrix composites. Scientific Reports, 2016, 6, 19363.	3.3	126
17	Achieving high strength and high ductility in metal matrix composites reinforced with a discontinuous three-dimensional graphene-like network. Nanoscale, 2017, 9, 11929-11938.	5.6	126
18	Effect of minor Sc and Zr on recrystallization behavior and mechanical properties of novel Al–Zn–Mg–Cu alloys. Journal of Alloys and Compounds, 2016, 657, 717-725.	5.5	125

#	Article	IF	CITATIONS
19	Effect of carbon nanotube (CNT) content on the properties of in-situ synthesis CNT reinforced Al composites. Materials Science & Engineering A: Structural Materials: Properties, Microstructure and Processing, 2016, 660, 11-18.	5.6	121
20	Designed synthesis of NiCo-LDH and derived sulfide on heteroatom-doped edge-enriched 3D rivet graphene films for high-performance asymmetric supercapacitor and efficient OER. Journal of Materials Chemistry A, 2018, 6, 8109-8119.	10.3	121
21	Metal–organic frameworks-derived honeycomb-like Co3O4/three-dimensional graphene networks/Ni foam hybrid as a binder-free electrode for supercapacitors. Journal of Alloys and Compounds, 2017, 693, 16-24.	5.5	120
22	Mo2C coating on diamond: Different effects on thermal conductivity of diamond/Al and diamond/Cu composites. Applied Surface Science, 2017, 402, 372-383.	6.1	117
23	In-situ synthesis of graphene decorated with nickel nanoparticles for fabricating reinforced 6061Al matrix composites. Materials Science & Engineering A: Structural Materials: Properties, Microstructure and Processing, 2017, 699, 185-193.	5.6	108
24	Sandwiched C@SnO ₂ @C hollow nanostructures as an ultralong-lifespan high-rate anode material for lithium-ion and sodium-ion batteries. Journal of Materials Chemistry A, 2017, 5, 10946-10956.	10.3	107
25	Capacitance controlled, hierarchical porous 3D ultra-thin carbon networks reinforced prussian blue for high performance Na-ion battery cathode. Nano Energy, 2019, 58, 192-201.	16.0	100
26	Free-Standing Porous Carbon Nanofiber/Ultrathin Graphite Hybrid for Flexible Solid-State Supercapacitors. ACS Nano, 2015, 9, 481-487.	14.6	99
27	Effect of Interface Structure on the Mechanical Properties of Graphene Nanosheets Reinforced Copper Matrix Composites. ACS Applied Materials & Interfaces, 2018, 10, 37586-37601.	8.0	99
28	Soluble salt self-assembly-assisted synthesis of three-dimensional hierarchical porous carbon networks for supercapacitors. Journal of Materials Chemistry A, 2015, 3, 22266-22273.	10.3	98
29	Salt-template-assisted synthesis of robust 3D honeycomb-like structured MoS ₂ and its application as a lithium-ion battery anode. Journal of Materials Chemistry A, 2016, 4, 8734-8741.	10.3	96
30	Three-Dimensional Network of N-Doped Carbon Ultrathin Nanosheets with Closely Packed Mesopores: Controllable Synthesis and Application in Electrochemical Energy Storage. ACS Applied Materials & Interfaces, 2016, 8, 11720-11728.	8.0	93
31	Preparation of reduced graphene oxide/Fe3O4 nanocomposite and its microwave electromagnetic properties. Materials Letters, 2013, 91, 209-212.	2.6	92
32	Fabrication of carbon nanotube reinforced Al composites with well-balanced strength and ductility. Journal of Alloys and Compounds, 2013, 563, 216-220.	5.5	89
33	Facile synthesis of 3D few-layered MoS ₂ coated TiO ₂ nanosheet core–shell nanostructures for stable and high-performance lithium-ion batteries. Nanoscale, 2015, 7, 12895-12905.	5.6	85
34	Artificial neural network enabled capacitance prediction for carbon-based supercapacitors. Materials Letters, 2018, 233, 294-297.	2.6	81
35	In-situ space-confined synthesis of well-dispersed three-dimensional graphene/carbon nanotube hybrid reinforced copper nanocomposites with balanced strength and ductility. Composites Part A: Applied Science and Manufacturing, 2017, 103, 178-187.	7.6	76
36	Scalable synthesis of high-quality transition metal dichalcogenide nanosheets and their application as sodium-ion battery anodes. Journal of Materials Chemistry A, 2016, 4, 17370-17380.	10.3	72

#	Article	IF	CITATIONS
37	First-principles study of protonic conduction in In-doped AZrO3 (A=Ca, Sr, Ba). Solid State Ionics, 2005, 176, 1091-1096.	2.7	70
38	In-situ organic SEI layer for dendrite-free lithium metal anode. Energy Storage Materials, 2020, 27, 69-77.	18.0	70
39	Freeâ€Standing 3D Nanoporous Duct‣ike and Hierarchical Nanoporous Graphene Films for Micron‣evel Flexible Solidâ€State Asymmetric Supercapacitors. Advanced Energy Materials, 2016, 6, 1600755.	19.5	66
40	Anomalous Interfacial Lithium Storage in Graphene/TiO ₂ for Lithium Ion Batteries. ACS Applied Materials & Interfaces, 2014, 6, 18147-18151.	8.0	65
41	Monodisperse multicore-shell SnSb@SnOx/SbOx@C nanoparticles space-confined in 3D porous carbon networks as high-performance anode for Li-ion and Na-ion batteries. Chemical Engineering Journal, 2019, 371, 356-365.	12.7	65
42	In situ synthesis of CNTs in Mg powder at low temperature for fabricating reinforced Mg composites. Journal of Alloys and Compounds, 2013, 551, 496-501.	5.5	62
43	Revealing the strengthening and toughening mechanisms of Al-CuO composite fabricated via in-situ solid-state reaction. Acta Materialia, 2021, 204, 116524.	7.9	62
44	Enhanced electrochemical hydrogen storage capacity of multi-walled carbon nanotubes by TiO2 decoration. International Journal of Hydrogen Energy, 2011, 36, 6739-6743.	7.1	60
45	Constructing N-Doped porous carbon confined FeSb alloy nanocomposite with Fe-N-C coordination as a universal anode for advanced Na/K-ion batteries. Chemical Engineering Journal, 2020, 384, 123327.	12.7	60
46	Low-temperature synthesis of carbon onions by chemical vapor deposition using a nickel catalyst supported on aluminum. Scripta Materialia, 2006, 54, 689-693.	5.2	59
47	Synthesis of uniformly dispersed carbon nanotube reinforcement in Al powder for preparing reinforced Al composites. Composites Part A: Applied Science and Manufacturing, 2011, 42, 1833-1839.	7.6	56
48	Electrochemical hydrogen storage of expanded graphite decorated with TiO2 nanoparticles. International Journal of Hydrogen Energy, 2012, 37, 5762-5768.	7.1	56
49	A large ultrathin anatase TiO2 nanosheet/reduced graphene oxide composite with enhanced lithium storage capability. Journal of Materials Chemistry A, 2014, 2, 8893.	10.3	56
50	Continuously hierarchical nanoporous graphene film for flexible solid-state supercapacitors with excellent performance. Nano Energy, 2016, 24, 158-164.	16.0	56
51	Yolk-shelled Sb@C nanoconfined nitrogen/sulfur co-doped 3D porous carbon microspheres for sodium-ion battery anode with ultralong high-rate cycling. Nano Energy, 2019, 66, 104133.	16.0	56
52	Fabrication of Nanocarbon Composites Using In Situ Chemical Vapor Deposition and Their Applications. Advanced Materials, 2015, 27, 5422-5431.	21.0	55
53	Thermogravimetric analysis and TEM characterization of the oxidation and defect sites of carbon nanotubes synthesized by CVD of methane. Materials Science & Engineering A: Structural Materials: Properties, Microstructure and Processing, 2008, 473, 355-359.	5.6	54
54	Hydrogen spillover storage on Ca-decorated graphene. International Journal of Hydrogen Energy, 2012, 37, 11835-11841.	7.1	53

#	Article	IF	CITATIONS
55	N-Doped Porous Carbon Nanofibers/Porous Silver Network Hybrid for High-Rate Supercapacitor Electrode. ACS Applied Materials & amp; Interfaces, 2017, 9, 30832-30839.	8.0	53
56	In-situ synthesis of graphene nanosheets coated copper for preparing reinforced aluminum matrix composites. Materials Science & Engineering A: Structural Materials: Properties, Microstructure and Processing, 2018, 709, 65-71.	5.6	52
57	Microwave absorbing properties of activated carbon fibre polymer composites. Bulletin of Materials Science, 2011, 34, 75-79.	1.7	51
58	Elevated temperature compressive properties and energy absorption response of in-situ grown CNT-reinforced Al composite foams. Materials Science & Engineering A: Structural Materials: Properties, Microstructure and Processing, 2017, 690, 294-302.	5.6	51
59	Facile synthesis and electrochemical properties of continuous porous spheres assembled from defect-rich, interlayer-expanded, and few-layered MoS2/C nanosheets for reversible lithium storage. Journal of Power Sources, 2018, 387, 16-23.	7.8	51
60	Effects of anodizing conditions on anodic alumina structure. Journal of Materials Science, 2007, 42, 3878-3882.	3.7	50
61	Effect of Ni, Fe and Fe-Ni alloy catalysts on the synthesis of metal contained carbon nano-onions and studies of their electrochemical hydrogen storage properties. Journal of Energy Chemistry, 2014, 23, 324-330.	12.9	50
62	Synergistic effect of CNTs reinforcement and precipitation hardening in in-situ CNTs/Al–Cu composites. Materials Science & Engineering A: Structural Materials: Properties, Microstructure and Processing, 2015, 633, 103-111.	5.6	50
63	Heterostructure Engineering of Coreâ€5helled Sb@Sb ₂ O ₃ Encapsulated in 3D Nâ€Doped Carbon Hollowâ€5pheres for Superior Sodium/Potassium Storage. Small, 2021, 17, e2006824.	10.0	49
64	In situ synthesis of a gamma-Al2O3 whisker reinforced aluminium matrix composite by cold pressing and sintering. Materials Science & Engineering A: Structural Materials: Properties, Microstructure and Processing, 2018, 709, 223-231.	5.6	48
65	In-situ grown CNTs modified SiO 2 /C composites as anode with improved cycling stability and rate capability for lithium storage. Applied Surface Science, 2018, 433, 428-436.	6.1	47
66	Ultrafine SnO2 nanoparticles encapsulated in 3D porous carbon as a high-performance anode material for potassium-ion batteries. Journal of Power Sources, 2019, 441, 227191.	7.8	47
67	A novel approach to obtain in-situ growth carbon nanotube reinforced aluminum foams with enhanced properties. Materials Letters, 2015, 161, 763-766.	2.6	46
68	Electronic reconfiguration of Co ₂ P induced by Cu doping enhancing oxygen reduction reaction activity in zinc–air batteries. Journal of Materials Chemistry A, 2019, 7, 21232-21243.	10.3	46
69	Enhanced Hydrogen Evolution Reaction Performance of NiCo ₂ P by Filling Oxygen Vacancies by Phosphorus in Thin-Coating CeO ₂ . ACS Applied Materials & Interfaces, 2019, 11, 32460-32468.	8.0	46
70	NiO nanotubes assembled in pores of porous anodic alumina and their optical absorption properties. Chemical Physics Letters, 2008, 454, 75-79.	2.6	44
71	In situ synthesis of high content graphene nanoplatelets reinforced Cu matrix composites with enhanced thermal conductivity and tensile strength. Powder Technology, 2020, 362, 126-134.	4.2	44
72	In-situ Al2O3-Al interface contribution towards the strength-ductility synergy of Al-CuO composite fabricated by solid-state reactive sintering. Scripta Materialia, 2021, 198, 113825.	5.2	44

#	Article	IF	CITATIONS
73	Spatially uniform Li deposition realized by 3D continuous duct-like graphene host for high energy density Li metal anode. Carbon, 2020, 161, 198-205.	10.3	43
74	Bamboo-shaped carbon nanotubes produced by catalytic decomposition of methane over nickel nanoparticles supported on aluminum. Journal of Alloys and Compounds, 2007, 428, 79-83.	5.5	42
75	Synthesis of carbon nanotubes and carbon onions by CVD using a Ni/Y catalyst supported on copper. Materials Science & Engineering A: Structural Materials: Properties, Microstructure and Processing, 2008, 475, 136-140.	5.6	42
76	Synthesis of uniform and superparamagnetic Fe3O4 nanocrystals embedded in a porous carbon matrix for a superior lithium ion battery anode. Journal of Materials Chemistry A, 2013, 1, 11011.	10.3	42
77	Compressive properties and energy absorption of aluminum composite foams reinforced by in-situ generated MgAl 2 O 4 whiskers. Materials Science & Engineering A: Structural Materials: Properties, Microstructure and Processing, 2015, 645, 1-7.	5.6	42
78	Space-Confined Synthesis of Three-Dimensional Boron/Nitrogen-Doped Carbon Nanotubes/Carbon Nanosheets Line-in-Wall Hybrids and Their Electrochemical Energy Storage Applications. Electrochimica Acta, 2016, 212, 621-629.	5.2	42
79	Sandwiched graphene inserted with graphene-encapsulated yolk–shell γ-Fe2O3 nanoparticles for efficient lithium ion storage. Journal of Materials Chemistry A, 2017, 5, 7035-7042.	10.3	42
80	ZnO nanoconfined 3D porous carbon composite microspheres to stabilize lithium nucleation/growth for high-performance lithium metal anodes. Journal of Materials Chemistry A, 2019, 7, 19442-19452.	10.3	42
81	An in-plane Co ₉ S ₈ @MoS ₂ heterostructure for the hydrogen evolution reaction in alkaline media. Nanoscale, 2019, 11, 21479-21486.	5.6	42
82	Adhesion, bonding and mechanical properties of Mo doped diamond/Al (Cu) interfaces: A first principles study. Applied Surface Science, 2020, 527, 146817.	6.1	41
83	Graphene Oxide-Assisted Synthesis of Microsized Ultrathin Single-Crystalline Anatase TiO ₂ Nanosheets and Their Application in Dye-Sensitized Solar Cells. ACS Applied Materials & Interfaces, 2016, 8, 2495-2504.	8.0	40
84	Interface and Doping Effects on Li Ion Storage Behavior of Graphene/Li ₂ O. Journal of Physical Chemistry C, 2017, 121, 19559-19567.	3.1	40
85	Formation of the orientation relationship-dependent interfacial carbide in Al matrix composite affected by architectured carbon nanotube. Acta Materialia, 2022, 228, 117758.	7.9	40
86	"Ethanol–water exchange―nanobubbles templated hierarchical hollow β-Mo ₂ C/N-doped carbon composite nanospheres as an efficient hydrogen evolution electrocatalyst. Journal of Materials Chemistry A, 2018, 6, 6054-6064.	10.3	39
87	In situ preparation of interconnected networks constructed by using flexible graphene/Sn sandwich nanosheets for high-performance lithium-ion battery anodes. Journal of Materials Chemistry A, 2015, 3, 23170-23179.	10.3	38
88	Bio-inspired three-dimensional carbon network with enhanced mass-transfer ability for supercapacitors. Carbon, 2019, 143, 728-735.	10.3	38
89	Synthesis of SiO2/3D porous carbon composite as anode material with enhanced lithium storage performance. Chemical Physics Letters, 2016, 651, 19-23.	2.6	37
90	Ball-in-cage nanocomposites of metal–organic frameworks and three-dimensional carbon networks: synthesis and capacitive performance. Nanoscale, 2017, 9, 6478-6485.	5.6	37

#	Article	IF	CITATIONS
91	Synthesis and growth mechanism of metal filled carbon nanostructures by CVD using Ni/Y catalyst supported on copper. Journal of Alloys and Compounds, 2008, 456, 290-296.	5.5	36
92	Synthesis of three-dimensional carbon networks decorated with Fe3O4 nanoparticles as lightweight and broadband electromagnetic wave absorber. Journal of Alloys and Compounds, 2019, 776, 691-701.	5.5	36
93	Phosphorus doping of 3D structural MoS2 to promote catalytic activity for lithium-sulfur batteries. Chemical Engineering Journal, 2022, 431, 133923.	12.7	36
94	Damping characteristics of Al matrix composite foams reinforced by in-situ grown carbon nanotubes. Materials Letters, 2017, 209, 68-70.	2.6	35
95	Enhanced mechanical properties and electrical conductivity of graphene nanoplatelets/Cu composites by in situ formation of Mo2C nanoparticles. Materials Science & Engineering A: Structural Materials: Properties, Microstructure and Processing, 2019, 766, 138365.	5.6	35
96	Towards strength-ductility synergy with favorable strengthening effect through the formation of a quasi-continuous graphene nanosheets coated Ni structure in aluminum matrix composite. Materials Science & amp; Engineering A: Structural Materials: Properties, Microstructure and Processing, 2019, 748, 52-58.	5.6	35
97	Nitrogen-doped graphene network supported copper nanoparticles encapsulated with graphene shells for surface-enhanced Raman scattering. Nanoscale, 2015, 7, 17079-17087.	5.6	32
98	In situ synthesized Li2S@porous carbon cathode for graphite/Li2S full cells using ether-based electrolyte. Electrochimica Acta, 2017, 256, 348-356.	5.2	32
99	In-situ fabrication of nano-sized TiO2 reinforced Cu matrix composites with well-balanced mechanical properties and electrical conductivity. Powder Technology, 2017, 321, 66-73.	4.2	32
100	Design of conical hollow ZnS arrays vertically grown on carbon fibers for lightweight and broadband flexible absorbers. Journal of Colloid and Interface Science, 2022, 607, 1287-1299.	9.4	32
101	Comprehensive performance regulation of Cu matrix composites with graphene nanoplatelets in situ encapsulated Al2O3 nanoparticles as reinforcement. Carbon, 2022, 188, 81-94.	10.3	32
102	Fabrication of aluminum matrix composites with enhanced mechanical properties reinforced by in situ generated MgAl2O4 whiskers. Composites Part A: Applied Science and Manufacturing, 2012, 43, 631-634.	7.6	31
103	Synthesis of carbon nanostructures with different morphologies by CVD of methane. Materials Science & Engineering A: Structural Materials: Properties, Microstructure and Processing, 2007, 460-461, 255-260.	5.6	30
104	Achieving highly dispersed nanofibres at high loading in carbon nanofibre–metal composites. Nanotechnology, 2009, 20, 235607.	2.6	30
105	Achieving prominent strengthening efficiency of graphene nanosheets in Al matrix composites by hybrid deformation. Carbon, 2021, 183, 530-545.	10.3	30
106	Microstructure and properties of in situ generated MgAl2O4 spinel whisker reinforced aluminum matrix composites. Materials & Design, 2013, 46, 724-730.	5.1	29
107	Microstructural evolution in Al-Zn-Mg-Cu-Sc-Zr alloys during short-time homogenization. International Journal of Minerals, Metallurgy and Materials, 2015, 22, 516-523.	4.9	29
108	Effect of Hydrogen Molecule Dissociation on Hydrogen Storage Capacity of Graphene with Metal Atom Decorated. Journal of Physical Chemistry C, 2014, 118, 839-844.	3.1	28

#	Article	IF	CITATIONS
109	High strain rate dynamic compressive properties and deformation behavior of Al matrix composite foams reinforced by in-situ grown carbon nanotubes. Materials Science & Engineering A: Structural Materials: Properties, Microstructure and Processing, 2018, 729, 487-495.	5.6	28
110	Engineering Pocketâ€Like Graphene–Shell Encapsulated FeS ₂ : Inhibiting Polysulfides Shuttle Effect in Potassiumâ€Ion Batteries. Advanced Functional Materials, 2022, 32, .	14.9	28
111	Carbon-coated Ni ₃ Sn ₂ nanoparticles embedded in porous carbon nanosheets as a lithium ion battery anode with outstanding cycling stability. RSC Advances, 2014, 4, 49247-49256.	3.6	27
112	Three-dimensional porous bowl-shaped carbon cages interspersed with carbon coated Ni–Sn alloy nanoparticles as anode materials for high-performance lithium-ion batteries. New Journal of Chemistry, 2017, 41, 393-402.	2.8	26
113	High-strength graphene network reinforced copper matrix composites achieved by architecture design and grain structure regulation. Materials Science & Engineering A: Structural Materials: Properties, Microstructure and Processing, 2019, 762, 138063.	5.6	26
114	Ultralight metal foams. Scientific Reports, 2015, 5, 13825.	3.3	25
115	Activated Carbon Nanochains with Tailored Micro-Meso Pore Structures and Their Application for Supercapacitors. Journal of Physical Chemistry C, 2015, 119, 21810-21817.	3.1	25
116	Preparation of Fe 3 O 4 /rebar graphene composite via solvothermal route as binder free anode for lithium ion batteries. Journal of Alloys and Compounds, 2016, 661, 448-454.	5.5	25
117	Carbon and few-layer MoS2 nanosheets co-modified TiO2 nanosheets with enhanced electrochemical properties for lithium storage. Rare Metals, 2018, 37, 107-117.	7.1	25
118	Ultrafine Ni(OH)2 nanoneedles on N-doped 3D rivet graphene film for high-performance asymmetric supercapacitor. Journal of Alloys and Compounds, 2019, 783, 625-632.	5.5	25
119	In-situ synthesis of CNTs@Al2O3 wrapped structure in aluminum matrix composites with balanced strength and toughness. Materials Science & Engineering A: Structural Materials: Properties, Microstructure and Processing, 2020, 797, 140058.	5.6	25
120	Effect of rare metal element interfacial modulation in graphene/Cu composite with high strength, high ductility and good electrical conductivity. Applied Surface Science, 2020, 533, 147489.	6.1	25
121	Understanding the Electrochemical Properties of Li-Rich Cathode Materials from First-Principles Calculations. Journal of Physical Chemistry C, 2015, 119, 28749-28756.	3.1	24
122	Multi-functional integration of pore P25@C@MoS2 core-double shell nanostructures as robust ternary anodes with enhanced lithium storage properties. Applied Surface Science, 2017, 401, 232-240.	6.1	24
123	Orientation Relationships and Interface Structure in MgAl ₂ O ₄ and MgAlB ₄ Co-Reinforced Al Matrix Composites. ACS Applied Materials & Interfaces, 2019, 11, 42790-42800.	8.0	24
124	Effects of active elements on adhesion of the Al2O3/Fe interface: A first principles calculation. Computational Materials Science, 2021, 188, 110226.	3.0	24
125	Exceptional mechanical properties of aluminum matrix composites with heterogeneous structure induced by in-situ graphene nanosheet-Cu hybrids. Composites Part B: Engineering, 2022, 234, 109731.	12.0	24
126	Smart hybridization of Sn ₂ Nb ₂ O ₇ /SnO ₂ @3D carbon nanocomposites with enhanced sodium storage performance through self-buffering effects. Journal of Materials Chemistry A, 2017, 5, 13052-13061.	10.3	23

#	Article	IF	CITATIONS
127	Boron doping effect on the interface interaction and mechanical properties of graphene reinforced copper matrix composite. Applied Surface Science, 2017, 425, 811-822.	6.1	23
128	Fabrication of in-situ grown carbon nanotubes reinforced aluminum alloy matrix composite foams based on powder metallurgy method. Materials Letters, 2018, 233, 351-354.	2.6	23
129	ReS2 nanosheets anchored on rGO as an efficient polysulfides immobilizer and electrocatalyst for Li-S batteries. Applied Surface Science, 2020, 505, 144586.	6.1	23
130	Two Birds with One Stone: A NaCl-Assisted Strategy toward MoTe2 Nanosheets Nanoconfined in 3D Porous Carbon Network for Sodium-Ion Battery Anode. Energy Storage Materials, 2022, 47, 591-601.	18.0	23
131	Nitrogen and oxygen co-doped 3D nanoporous duct-like graphene@carbon nano-cage hybrid films for high-performance multi-style supercapacitors. Journal of Materials Chemistry A, 2017, 5, 18535-18541.	10.3	22
132	Nanotubular Ni-supported graphene @ hierarchical NiCo-LDH with ultrahigh volumetric capacitance for supercapacitors. Applied Surface Science, 2018, 453, 230-237.	6.1	22
133	Compressive responses and strengthening mechanisms of aluminum composite foams reinforced with graphene nanosheets. Carbon, 2019, 153, 396-406.	10.3	22
134	Covalently bonded 3D rebar graphene foam for ultrahigh-areal-capacity lithium-metal anodes by in-situ loose powder metallurgy synthesis. Carbon, 2020, 158, 536-544.	10.3	22
135	Doping effects on proton incorporation and conduction in SrZrO3. Journal of Computational Chemistry, 2006, 27, 711-718.	3.3	21
136	Microwave absorbing properties of activated carbon-fiber felt dipole array/epoxy resin composites. Journal of Materials Science, 2007, 42, 4870-4876.	3.7	21
137	Low-temperature synthesis of aluminum borate nanowhiskers on the surface of aluminum powder promoted by ball-milling pretreatment. Powder Technology, 2011, 212, 310-315.	4.2	21
138	Interface and Doping Effect on the Electrochemical Property of Graphene/LiFePO ₄ . Journal of Physical Chemistry C, 2016, 120, 17165-17174.	3.1	21
139	Rational design of FeCo imbedded 3D porous carbon microspheres as broadband and lightweight microwave absorbers. Journal of Materials Science, 2021, 56, 2212-2225.	3.7	21
140	Hierarchical nickle-iron layered double hydroxide composite electrocatalyst for efficient oxygen evolution reaction. Materials Today Nano, 2022, 17, 100150.	4.6	21
141	Three-dimensional porous carbon nanosheet networks anchored with Cu ₆ Sn ₅ @carbon as a high-performance anode material for lithium ion batteries. RSC Advances, 2016, 6, 54718-54726.	3.6	20
142	Single-Atom Cobalt Supported on Nitrogen-Doped Three-Dimensional Carbon Facilitating Polysulfide Conversion in Lithium–Sulfur Batteries. ACS Applied Materials & Interfaces, 2022, 14, 25337-25347.	8.0	20
143	In-situ synthesis of MgAl2O4 nanowhiskers reinforced 6061 aluminum alloy composites by reaction hot pressing. Materials Science & Engineering A: Structural Materials: Properties, Microstructure and Processing, 2014, 617, 235-242.	5.6	19
144	Synthesis of binary and triple carbon nanotubes over Ni/Cu/Al2O3 catalyst by chemical vapor deposition. Materials Letters, 2007, 61, 4940-4943.	2.6	18

#	Article	IF	CITATIONS
145	In-situ processing and aging behaviors of MgAl2O4 spinel whisker reinforced 6061Al composite. Materials Science & Engineering A: Structural Materials: Properties, Microstructure and Processing, 2014, 598, 114-121.	5.6	18
146	Interface intrinsic strengthening mechanism on the tensile properties of Al2O3/Al composites. Computational Materials Science, 2019, 169, 109131.	3.0	18
147	In-situ synthesis of MgAlB4 whiskers as a promising reinforcement for aluminum matrix composites. Materials Science & Engineering A: Structural Materials: Properties, Microstructure and Processing, 2019, 764, 138229.	5.6	17
148	Synthesis of novel carbon nano-chains and their application as supercapacitors. Journal of Materials Chemistry A, 2014, 2, 16268-16275.	10.3	16
149	Carbon onion growth enhanced by nitrogen incorporation. Scripta Materialia, 2006, 54, 1739-1743.	5.2	15
150	MnO nanoparticles@continuous carbon nanosheets for high performance lithium ion battery anodes. Materials Letters, 2017, 189, 236-239.	2.6	15
151	Synthesis of 2D/3D carbon hybrids by heterogeneous space-confined effect for electrochemical energy storage. Journal of Materials Chemistry A, 2017, 5, 19175-19183.	10.3	15
152	Dopant-Modulating Mechanism of Lithium Adsorption and Diffusion at the Graphene/Li2S Interface. Physical Review Applied, 2018, 9, .	3.8	15
153	Hydrogen bonding regulation enables indanthrone as a stable and high-rate cathode for lithium-ion batteries. Energy Storage Materials, 2022, 51, 172-180.	18.0	15
154	The effect of heat treatment on mechanical properties of carbon nanofiber reinforced copper matrix composites. Journal of Materials Science, 2009, 44, 5602-5608.	3.7	14
155	An approach for obtaining the structural diversity of multi-walled carbon nanotubes on Ni/Al catalyst with low Ni content. Journal of Alloys and Compounds, 2010, 489, 20-25.	5.5	14
156	First-principles study of the B- or N-doping effects on chemical bonding characteristics between magnesium and single-walled carbon nanotubes. Chemical Physics Letters, 2009, 469, 145-148.	2.6	13
157	Surface State Induced Ferromagnetism in Co- and Mn-Doped ZnO Surfaces. Journal of Physical Chemistry C, 2011, 115, 3368-3371.	3.1	13
158	Preparation and mechanical properties of in-situ synthesized nano-MgAl2O4 particles and MgxAl(1-x)B2 whiskers co-reinforced Al matrix composites. Materials Science & Engineering A: Structural Materials: Properties, Microstructure and Processing, 2018, 735, 236-242.	5.6	13
159	Enhanced Shielding Performance of Layered Carbon Fiber Composites Filled with Carbonyl Iron and Carbon Nanotubes in the Koch Curve Fractal Method. Molecules, 2020, 25, 969.	3.8	13
160	Low-temperature synthesis of multi-walled carbon nanotubes over Cu catalyst. Materials Letters, 2012, 72, 164-167.	2.6	12
161	Octopus-Inspired Design of Apical NiS ₂ Nanoparticles Supported on Hierarchical Carbon Composites as an Efficient Host for Lithium Sulfur Batteries with High Sulfur Loading. ACS Applied Materials & Interfaces, 2020, 12, 17528-17537.	8.0	12
162	Interface modulation mechanism of alloying elements on the interface interaction and mechanical properties of graphene/copper composites. Applied Surface Science, 2022, 571, 151314.	6.1	12

#	Article	IF	CITATIONS
163	Simultaneously optimizing pore morphology and enhancing mechanical properties of Al-Si alloy composite foams by graphene nanosheets. Journal of Materials Science and Technology, 2022, 101, 60-70.	10.7	12
164	Doping and controllable pore size enhanced electrochemical performance of free-standing 3D graphene films. Applied Surface Science, 2018, 427, 598-604.	6.1	11
165	Synthesis of interconnected carbon nanosheets anchored with Fe3O4 nanoparticles as broadband electromagnetic wave absorber. Chemical Physics Letters, 2019, 716, 221-226.	2.6	11
166	High strength-ductility synergy of MgAlB4 whisker reinforced aluminum matrix composites achieved by in situ synthesis. Materials Science & Engineering A: Structural Materials: Properties, Microstructure and Processing, 2021, 799, 140127.	5.6	11
167	Ultrafine Fe3N nanocrystals coupled with N doped 3D porous carbon networks induced atomically dispersed Fe for superior sodium ion storage. Carbon, 2022, 196, 795-806.	10.3	11
168	Simultaneously enhanced mechanical properties and electrical property of Cu-2 wt% Ag alloy matrix composites with analogy-bicontinuous structures constructed via in-situ synthesized graphene nanoplatelets. Carbon, 2022, 198, 207-218.	10.3	11
169	The effect of catalyst evolution at various temperatures on carbon nanostructures formed by chemical vapor deposition. Journal of Materials Science, 2009, 44, 2471-2476.	3.7	10
170	Self-anchored catalysts for substrate-free synthesis of metal-encapsulated carbon nano-onions and study of their magnetic properties. Nano Research, 2016, 9, 1159-1172.	10.4	10
171	Hetero-structure effect on Na adsorption and diffusion in two dimensional composites. Electrochimica Acta, 2018, 285, 309-316.	5.2	10
172	Ultrahigh volumetric capacitance and cycle stability via structure design and synergistic action between CoMoO4 nanosheets and 3D porous Ni-Co film. Applied Surface Science, 2019, 465, 389-396.	6.1	10
173	Comparison of electronic structures and mechanical properties of MgAlB4, AlB2 and MgB2 using first-principles calculations. Ceramics International, 2020, 46, 12548-12558.	4.8	10
174	Graphene oxide supported YolkÂâ´`ÂShell ZnS/Ni3S4 with the adjustable air layer for high performance of electromagnetic wave absorber. Journal of Colloid and Interface Science, 2022, 617, 620-632.	9.4	10
175	Fabrication and performance of SiC-reinforced Cu: Role of the aspect ratio of the SiC reinforcement phase. Materials and Design, 2022, 220, 110869.	7.0	10
176	Adsorption of hydrogen atoms on graphene with TiO2 decoration. Journal of Applied Physics, 2013, 113, 153708.	2.5	9
177	Fabrication of Carbon Nanotube-Reinforced 6061Al Alloy Matrix Composites by an In Situ Synthesis Method Combined with Hot Extrusion Technique. Acta Metallurgica Sinica (English Letters), 2016, 29, 188-198.	2.9	9
178	Synergistic strengthening effect of alumina anchored graphene nanosheets hybrid structure in aluminum matrix composites. Fullerenes Nanotubes and Carbon Nanostructures, 2019, 27, 640-649.	2.1	9
179	Boosting the charge transfer efficiency of metal oxides/carbon nanotubes composites through interfaces control. Journal of Power Sources, 2021, 489, 229501.	7.8	9
180	Synthesis of carbon nanohorns by the simple catalytic method. Journal of Alloys and Compounds, 2009, 473, 288-292.	5.5	8

#	Article	IF	CITATIONS
181	A Chemical-Adsorption Strategy to Enhance the Reaction Kinetics of Lithium-Rich Layered Cathodes via Double-Shell Surface Modification. ACS Applied Materials & Interfaces, 2016, 8, 24594-24602.	8.0	8
182	Assembly Multifunctional Three-Dimensional Carbon Networks by Controlling Intermolecular Forces. ACS Applied Materials & Interfaces, 2018, 10, 36284-36289.	8.0	7
183	Regulation of the interface binding and mechanical properties of TiB/Ti via doping-induced chemical and structural effects. Computational Materials Science, 2020, 174, 109506.	3.0	7
184	Enhanced interface interaction between modified carbon nanotubes and magnesium matrix. Composite Interfaces, 2018, 25, 1101-1114.	2.3	6
185	Interface bonding and mechanical properties of copper/graphene interface doped with rare earth elements: First principles calculations. Physica E: Low-Dimensional Systems and Nanostructures, 2022, 142, 115260.	2.7	6
186	Study of Mg Powder as Catalyst Carrier for the Carbon Nanotube Growth by CVD. Journal of Nanomaterials, 2011, 2011, 1-6.	2.7	5
187	Interfacial chemical bonding between carbon nanotube and aluminum substrate modulated by alloying elements. Diamond and Related Materials, 2015, 59, 1-6.	3.9	5
188	The preparation and properties of novel structural damping composites reinforced by nitrile rubber coated 3â€D braided carbon fibers. Polymer Composites, 2019, 40, E599.	4.6	5
189	W Clusters <i>In Situ</i> Assisted Synthesis of Layered Carbon Nanotube Arrays on Graphene Achieving High-Rate Performance. ACS Applied Materials & Interfaces, 2021, 13, 19117-19127.	8.0	5
190	Microstructure evolution and tensile behavior of MgAlB4w/Al composites at high temperatures. Journal of Alloys and Compounds, 2021, 884, 161088.	5.5	5
191	Cu–ion induced self-polymerization of Cu phthalocyanine to prepare low-cost organic cathode materials for Li-ion batteries with ultra-high voltage and ultra-fast rate capability. Journal of Materials Chemistry A, 2021, 9, 24915-24921.	10.3	5
192	General rules governing carbon nanomaterial growth directly on metal support by chemical vapor deposition. Materials Chemistry and Physics, 2011, 125, 386-389.	4.0	4
193	Compressive Response and Energy Absorption Characteristics of In Situ Grown CNTâ€Reinforced Al Composite Foams. Advanced Engineering Materials, 2017, 19, 1700431.	3.5	4
194	Microstructure and tensile properties of A356 alloy with different Sc/Zr additions. Rare Metals, 2021, 40, 2514-2522.	7.1	4
195	Electromagnetic and microwave absorbing properties of hollow carbon nanospheres. Bulletin of Materials Science, 2013, 36, 213-216.	1.7	3
196	Combined Effects of Pre-deformation and Pre-aging on the Mechanical Properties of Al-Cu-Mg Alloy with Sc and Zr Addition. Journal Wuhan University of Technology, Materials Science Edition, 2018, 33, 680-687.	1.0	3
197	Enhanced Cyclability of Cr8O21 Cathode for PEO-Based All-Solid-State Lithium-Ion Batteries by Atomic Layer Deposition of Al2O3. Materials, 2021, 14, 5380.	2.9	3
198	Lithiophilic Property of Artificial Alkoxides and Mercaptide Layers to Guide Uniform Li Nucleation for Stable Lithium Metal Anodes. Journal of Physical Chemistry C, 2021, 125, 22493-22501.	3.1	3

#	Article	IF	CITATIONS
199	Structure and photoluminescence of SiC/ZnO nanocomposites prepared by radio frequency alternate sputtering. Journal of Materials Science, 2010, 45, 6657-6660.	3.7	2
200	Phase Component-controllable Synthesis of Layered-Spinel Composite Materials as High-Performance Cathode for Lithium-ion Battery. Electrochemistry, 2016, 84, 407-413.	1.4	2
201	Defect Effects on the Interfacial Interactions between a (5, 5) Carbon Nanotube and an Al†(111) Surface. Zeitschrift Fur Physikalische Chemie, 2016, 230, 809-817.	2.8	2
202	Microstructural evolution and mechanical behavior of in situ synthesized MgAl2O4 whiskers reinforced 6061 Al alloy composite after hot extrusion and annealing. Rare Metals, 2018, , 1.	7.1	2
203	Regulation of the Interface Binding and Elastic Properties of SiC/Ti via Dopingâ€Induced Electronic Localization. Physica Status Solidi (B): Basic Research, 2020, 257, 1900163.	1.5	2
204	Three-Dimensional Carbon Networks Decorated with CoFe ₂ O ₄ Nanoparticles Composites: Fabrication and Broadband Electromagnetic Wave Absorption Performance. Integrated Ferroelectrics, 2020, 208, 164-176.	0.7	2
205	Preparation of Three-Dimensional Carbon Network Reinforced Epoxy Composites and Their Thermal Conductivity. Transactions of Tianjin University, 2020, 26, 399-408.	6.4	2
206	Balancing Strength and Ductility in Al Matrix Composites Reinforced by Few-Layered MoS2 through In-Situ Formation of Interfacial Al12Mo. Materials, 2021, 14, 3561.	2.9	2
207	Stress Relaxation Constitutive Relations and Finite Element Analysis of T9A Helical Compression Spring. Materials Transactions, 2021, 62, 962-967.	1.2	2
208	In Situ Internal Strengthened Carbon Nanotube Carpets on Graphene for Anti-Icing Application. ACS Applied Nano Materials, 2021, 4, 10952-10959.	5.0	2
209	Lithiophilic seeds and rigid arrays synergistic induced dendrite-free and stable Li anode towards long-life lithium-oxygen batteries. Journal of Energy Chemistry, 2022, 73, 268-276.	12.9	2
210	Preparation of 3YSZ/Cu composite by in-situ chemical route. Journal of Materials Science, 2007, 42, 5671-5675.	3.7	1
211	TiO2 cellular-protected nanowire array fabricated super-rapidly by the precipitation of colloids in the nanopores. Journal of Materials Chemistry, 2012, 22, 13820.	6.7	1
212	Supercapacitors: Free-Standing 3D Nanoporous Duct-Like and Hierarchical Nanoporous Graphene Films for Micron-Level Flexible Solid-State Asymmetric Supercapacitors (Adv. Energy Mater. 18/2016). Advanced Energy Materials, 2016, 6, .	19.5	1
213	Microwave absorption studies of the planar equiangular spiral antenna array/epoxy resin composites. Journal of Materials Science, 2009, 44, 2427-2429.	3.7	0